Agrobacterium-mediated *Cuscuta campestris* transformation as a tool for understanding plant-plant interactions

Supral Adhikari[1, †], Asha Mudalige[1, †], Lydia Phillips[1], Hyeyoung Lee[2], Vivian Bernal-Galeano[3], Hope Gruszewski[3], James H. Westwood[3], So-Yon Park*[1]

[1] Division of Plant Science and Technology, University of Missouri, Columbia, MO, 65211, USA

[2] Division of Animal Science, University of Missouri, Columbia, MO, 65211, USA

[3] School of Plant and Environmental Sciences, Virginia Tech, Blacksburg, VA, 24061, USA

*Author for correspondence: parksoy@missouri.edu

[†] These authors contributed equally to this article.

ORCIDs:

Supral Adhikari https://orcid.org/0000-0002-9914-2986

Asha Mudalige https://orcid.org/0009-0002-2842-1758

Lydia Phillips

Hyeyoung Lee

Vivian Bernal-Galeano https://orcid.org/0000-0002-0438-2937

Hope Gruszewski

James H. Westwood https://orcid.org/0000-0001-5127-7294

So-Yon Park https://orcid.org/0000-0002-2126-3382

Summary

Cuscuta campestris, a stem parasitic plant, has served as a valuable model plant for the exploration of plant-plant interactions and molecular trafficking. However, a major barrier to *C. campestris* research is that a method to generate stable transgenic plants has not yet been developed. Here, we describe the development of a *Cuscuta* transformation protocol using various reporter genes (GFP, GUS, or RUBY) and morphogenic genes (*CcWUS2* and *CcGRF/GIF*), ultimately leading to a robust protocol for *Agrobacterium*-mediated *C. campestris* transformation. The stably transformed and regenerated RUBY *C. campestris* plants produced haustoria, the signature organ of parasitic plants, and these were functional in forming host attachments. Transformed *C. campestris* also produced flowers and transgenic seeds exhibiting betalain pigment, providing proof of germline transmission of the RUBY transgene. The integration locations of T-DNAs were confirmed through TAIL-PCR. Furthermore, the RUBY reporter is not only a useful selectable marker for the *Agrobacterium*-mediated transformation but also provides insight into the movement of molecules from *C. campestris* to the host during parasitism. Thus, the protocol to generate transgenic *C. campestris* reported here overcomes a major obstacle to *Cuscuta* research and opens up new possibilities for studying parasitic plant interactions.

Key words: *Cuscuta*, parasitic plant, *Agrobacterium*-mediated transformation, plant-plant interactions, RUBY, mobile molecules.

Introduction

Cuscuta spp. are obligate stem parasitic plants that infect a broad range of host plants (Dawson *et al.*, 1994). The thread-like plant consists of leafless, twining stems that can attach to all aerial parts of herbaceous plants, woody shrubs, and even trees. The parasitic invasion of a *Cuscuta* begins by coiling around the stem of its host plant and initiating points of growth toward the host. The epidermal cells of the adhesive disk secrete a bioadhesive substance that anchors the parasite to the host (Vaughn, 2002; Galloway *et al.*, 2020). Next, a multicellular feeding structure termed the haustorium develops from the parasite stem and breaches the host tissues using a combination of mechanical pressure and enzymatic digestion of host cell walls, ultimately resulting in vascular connections with the host (Nagar *et al.*, 1984; Johnsen *et al.*, 2015; Kaiser *et al.*, 2015).

Cuscuta spp. are among the most agriculturally destructive parasitic weeds, as well as interesting subjects for studies of plant-plant interaction. The economic impact is due to their wide range of potential host species, which includes many dicotyledonous crops and ornamental plants (Lanini & Kogan, 2005), as well as their habit of extracting water and nutrients that the host needs for productivity. For example, *C. campestris* reduced tomato fresh weight by 98% in a greenhouse study (Goldwasser *et al.*, 2012), and *C. indecora* decreased alfalfa yield by 57% (Cudney *et al.*, 1992). Although systematic, chemical, and mechanical control methods have been developed to suppress the growth of *Cuscuta*, there is currently no efficient method to eliminate established *Cuscuta* without also causing damage to their hosts (Dechassa & Regassa, 2021).

Cuscuta spp. are useful for plant biology because their parasitic lifestyle provides insights into the mechanisms by which plants detect and interact with other plants. Examples of this include *Cuscuta* detection of neighboring plants by volatile signals (Runyon *et al.*, 2006), *Cuscuta*-to-host bidirectional mobility of mRNAs, small RNAs, and proteins (Kim *et al.*, 2014; Shahid *et al.*, 2018; Liu *et al.*, 2020; Park *et al.*, 2022), and elucidation of host resistance mechanisms against parasites (Hegenauer *et al.*, 2016; Hegenauer *et al.*, 2020). Therefore, both applied and basic plant sciences would benefit from greater ability to investigate the molecular mechanisms underlying interactions between *Cuscuta* and its hosts.

Plant genetic transformation is an essential tool for functional genomic studies as it enables the delivery of foreign genes to generate transgenic plants such as knockout or overexpression

mutant lines. This approach has been used for selected species of parasitic plants in the family Orobanchaceae to understand the mechanisms by which they develop and interact with their hosts. Methods for the transient and stable transformation of these root parasitic plants have been published for *Triphysaria versicolor, Phtheirospermum japonicum*, and *Phelipanche aegyptiaca* (Tomilov *et al.*, 2007; Fernández-Aparicio *et al.*, 2011; Ishida *et al.*, 2011; Bandaranayake & Yoder, 2018).

As for *Cuscuta* transformation, several efforts have led to partial success. Regeneration of shoots from callus of *C. reflexa* (Srivastava & Dwivedi, 2001) has been reported, and transformation was accomplished in cultured *C. trifolii* (Borsics *et al.*, 2002) and *C. europeae* (Švubová & Blehová, 2013). Transformation of haustorial structures was recently accomplished in *C. reflexa* (Lachner *et al.*, 2020). However, despite these attempts with diverse *Cuscuta* species, the inability to regenerate a functional *Cuscuta* plant from transformed explant tissues has blocked progress toward achieving stably transformed *Cuscuta*.

The failure to regenerate plants from transgenic callus is a common bottleneck in plant transformation, but progress has come from the use of genes involved in morphogenesis, which promote the formation of plant organs in callus of plant species that are recalcitrant to transformation or regeneration (Lee & Wang, 2023). For example, recent reports have shown improved regeneration and transformation efficiency with the representative morphogenic transcription factors such as *WUSCHEL* (*WUS*) and *BABY BOOM* (*BBM*). *WUS*, previously known to play a vital role in maintaining the stem cell population, was also found to enhance embryogenesis in *Arabidopsis* (Zuo *et al.*, 2002). When used with a transformation recalcitrant maize line, *BBM-WUS* enhanced transformation efficiency by over 40% (Lowe *et al.*, 2016). In another approach, a chimera consisting of *GROWTH-REGULATING FACTOR* (*GRF*) and its co-factor *GRF-INTERACTING FACTOR* (*GIF*) was shown to promote transformation and regeneration efficiency in wheat and citrus (Debernardi *et al.*, 2020). *GRF* and *GIF* are transcription factors regulating growth and development of plants, and their ability to enhance the efficiency of transformation has been extended to maize, watermelon, and lettuce. The combination of *GRF-GIF* with *BBM* improved the transformation efficiency of maize seedlings from 26% to 37% (Chen *et al.*, 2022). Furthermore, in watermelon, overexpression of the *GRF-GIF* chimeric gene resulted in higher transformation efficiency than control conditions (Feng *et*

109 *al.*, 2021). The *GRF-GIF* chimera with mutated miRNA396 improved the regeneration and
110 shooting efficiency in lettuce (Bull *et al.*, 2023).
111 Here we describe a transformation protocol for *C. campestris* that explored several different
112 reporter genes and morphogenic genes. Although *Cuscuta* species have been broadly regarded as
113 recalcitrant to transformation, the technique readily generates transgenic *C. campestris* plants
114 that show normal coiling and haustorium formation, and ultimately produce flowers and seeds.
115 This approach unlocks new possibilities for conducting functional studies on *Cuscuta* and
116 facilitates investigations into understanding of plant-plant interactions.
117

118 **Materials and methods**

119 ***Cuscuta* seed scarification and germination**

120 *C. campestris* seedlings were attached to 3-week-old beets (*Beta vulgaris*) and grown in a
121 greenhouse with a temperature of 25°C - 30°C and day/night length of 16/8 hours. Three months
122 after the inoculation, *Cuscuta* seeds were collected and cleaned. To promote germination, clean
123 seeds were scarified as described previously (Bernal-Galeano *et al.*, 2022). Scarified seeds were
124 rinsed with autoclaved water three times, stirred in 3% sodium hypochlorite solution for 15
125 minutes for the sterilization. The treated seeds were washed by autoclaved water five times and
126 incubated at 4C° overnight. For seed germination, 100 *Cuscuta* seeds were placed on a Petri dish
127 with a wet 3M paper and incubated in a 28C° incubator without light for two days. The Petri dish
128 containing *Cuscuta* seedlings was transferred to a walk-in chamber (25C° and 16 light/8 dark
129 light conditions) and incubated for one day.

130 ***Agrobacterium*-mediated *Cuscuta* transformation**

131 To develop a proper *Cuscuta* transformation protocol by *Agrobacterium*-mediated, we
132 conducted three different protocols, such as optimization of growth hormone concentration,
133 comparison of inoculation methods, and stable generation of *Cuscuta* transgenic lines.

134 First protocol-*Optimization of growth hormone concentration*: Starting with 3-day-old
135 seedlings (Figure 1A), the shoot apical meristem end and root were cut from each plant (Figure
136 1B), and submerged into liquid modified Murashige and Skoog (MMS) with *A. tumefaciens*
137 EHA105 harboring the construct *35S:GUS-pMAS:GFP* (Figure 1C and Supp table 1). The
138 hypocotyls were placed on MMS media containing 3 mg/L NAA and 1 mg/L BAP for co-
139 cultivation at 15 C° over 7 days with long-day condition (Figure 1D and Supp table 1)
140 (Srivastava & Dwivedi, 2001). Subsequently, the infected explants were transferred to MMS
141 media with the antibiotic cefotaxime and various types and concentrations of cytokinin and auxin
142 to further optimize the growth (Figure 1E).

143 Second protocol-*Optimization of growth hormone concentration*: Using a sterilized surgical
144 blade, 3-day-old seedlings were chopped into small pieces to make around 5mm segments,
145 which greatly facilitated the tissue preparation step and produce large number of transformable
146 sections at once. Also, instead of a construct with GUS and GFP reporters, we used a construct
147 containing *35S:RUBY* (He *et al.*, 2020). Transformed tissues expressing RUBY were counted
148 around a month after inoculation.

149 Third protocol-*Stable generation of Cuscuta transgenic lines*: Four-day-old *Cuscuta*
150 seedlings were chopped into small pieces as described in the second protocol. After cocultivation
151 with *A. tumefaciens* solutions, *Cuscuta* seedlings were uniformly distributed and incubated on
152 co-cultivation media for five days at 25 C° with long-day condition (Supp table 2). After the co-
153 cultivation stage, infected seedlings were transferred to Callus Induction Media (CIM)
154 containing 5 mg/L BAP and 250 mg/L Cefotaxime (Supp table 2). For the GUS staining assay,
155 calli were harvested 30-35 days after infection. To generate stably transformed *Cuscuta*, calli
156 were incubated on CIM for at least 8 weeks, shoot induction media (SIM) for 8 weeks, and shoot
157 elongation media for 3-4 weeks (Supp table 2).

158 **GUS staining and GFP observation**

159 For the GUS staining, *Cuscuta* calli were incubated in X-Gluc solution for up to 24 hours and
160 destained in 95 % Ethanol (Park *et al.*, 2022). For GFP detection, explants were placed on Laxco
161 stereomicroscope (Fisher) and observed with blue excitation light (Nightsea, SFA-RB-GO).

162 **Vibratome sectioning and imaging**

163 *Cuscuta* haustoria expressing RUBY grown on Rutgers tomatoes or *Arabidopsis* Col-0 were
164 harvested and embedded in 5 % Agarose (Park *et al.*, 2022). Tissue sectioning was performed
165 using a Leica series Vibratome 3000 Plus. Longitudinal and transverse sections were cut with
166 thickness ranging from 250µm to 400µm, depending on the softness of the tissue. Sections were
167 stained by 0.02% toluidine blue o (Pradhan Mitra & Loqué, 2014). For imaging, sections were
168 placed on microscope slides and imaged by Leica M205 FA automated stereo microscope.

169 **Thermal asymmetric interlaced (TAIL)-PCR**

170 To confirm T-DNA insertions in transgenic *Cuscuta*, genomic DNA was extracted using
171 Cetyltrimethylammonium-bromide (CTAB) (Sigma), and TAIL PCRs were conducted using
172 insertion specific primers (RB1 and RB2) and arbitrary degenerate primers (AD primers) (Supp
173 tables 3 and 4). Specific bands from amplification with AD and RB2 primers were extracted and
174 sequenced. The presence of T-DNA insertions in transgenic RUBY *Cuscuta* plants was verified
175 by aligning the sequencing results with a *Cuscuta campestris* genome sequence (Vogel et al.,
176 2018).

177 **Vector constructions**

178 *35S:GUS-pMAS:GFP* was modified by replacing the 35S promoter with the MAS promoter
179 from *pGFPGUSPlus* (Plasmid #64401, Addgene) (He *et al.*, 2020).

180 *CcGRF* and *CcGIF* were identified from the *C. campestris* genome (Vogel et al., 2018) via
181 sequence alignments and phylogenetic trees including wheat homologs (Debernardi et al., 2020),
182 performed in the Geneious Prime 2022.2.2 software. The selected *CcGRF* homolog Cc010427
183 and *CcGIF* homolog Cc021394 were cloned and sequenced using gene specific primers (Supp
184 table 5). The confirmed clones were ligated to make a *CcGRF/CcGIF* fusion via the Golden Gate
185 method using NEB's NEBridge kit and re-cloned into pCR8GWTOPO vector (Invitrogen).
186 *CcWUS2* was synthesized by Azenta life science (www.azenta.com) and re-cloned into
187 pCR8GWTOPO vector.
188 *CcWUS2* and *CcGRF/GIF* in entry clone pCR8GWTOPO were incubated with LR clonase
189 and pMDC139 to generate destination vectors with genes of interest (*35S:CcWUS2-GUS* and
190 *35S:CcGRF/CcGIF-GUS*). *35S:GUS-MAS:GFP*, *35S:CcWUS2-GUS*, and *35S:CcGRF/GIF-GUS*
191 were transformed to *A. tumefaciens* EHA105 strain.
192

Results

Test hormones and media compositions for *C. campestris* tissue culture

To establish the transformation protocol for *C. campestris*, we initially conducted screenings involving various concentrations of NAA and cytokinin (BAP/TDZ) in a medium designed for both co-cultivation and callus induction (Supp table 1). A negative control, consisting of the same medium without growth hormones, was also employed. GFP expression patterns were observed thirty days post-inoculation with *A. tumefaciens* EHA105-*35S:GUS-pMAS:GFP* (Figure 1). A callus showing fluorescence with the blue excitation light (Figure 1F) but not with the yellow excitation light (Figure 1G) was counted as transformed tissue (Supp table 6). Initially, we conducted a comparison of transformation efficiencies between groups with the presence or absence of plant growth regulators. The statistical analysis indicated a significantly higher GFP expression in the media containing plant growth regulators compared to that without hormones (Figure 2). *Cuscuta* calli cultivated on CIM media with BAP or TDZ exhibited significantly higher GFP expression than those on CIM media with NAA or the no hormone media, indicating that the presence of cytokinins (BAP or TDZ) had a noteworthy impact on efficiency. However, there was no significant difference among treatments with different concentration of BAP or TDZ. Thus, we concluded that the presence of BAP or TDZ without NAA in the CIM culture media significantly enhanced the *C. campestris* transformation efficiency. For further analysis, we used 5 mg/L BAP to induce *Cuscuta* callus in CIM media.

Comparing the cut *vs* the chop method using RUBY reporter

While approximately 50% of *Cuscuta* calli expressed GFP 30 days after *A. tumefaciens* inoculation and cultivated on 5mg/L BAP media (Figure 2), the preparation of individual meristems through the cut method (Figure 1B) is labor-intensive, as it involves the individual handling of each seedling. To simplify the inoculation process, we developed a bulk chopping method that is less precise but quicker and we conducted a comparative assessment of transformation efficiencies between the cut and bulk chop methods for preparing *Cuscuta* segments.

In this comparison, both cut and bulk chopped samples were infected with *A. tumefaciens* EHA105-*35S:RUBY* and incubated on MMS with 5mg/L BAP for 30 days. RUBY encodes enzymes for the synthesis of betalain and is useful for visually monitoring transformation events without extra equipment. Calli derived from the cut method exhibited 100% RUBY expression,

224 whereas calli from the bulk chop method displayed relatively lower RUBY expression (65%)
225 (Supp table 7). Previously we found that only the meristem region of *Cuscuta* was transformable
226 tissue, while neither the roots nor the shoots of *Cuscuta* exhibited such expression (Mudalige et
227 al., under preparation). Thus, we hypothesize that the bulk chop method had lower RUBY
228 expression than the cut method because the non-transformable tissues including root or shoot tips
229 were included with the transformable tissues incubated on the media. In addition, calli
230 expressing RUBY from the bulk chop method (Figure 3D-F) did not exhibit any phenotypic
231 differences when compared to calli from the cut method (Figure 3A-C). Even four-month-old
232 calli from the bulk chop method displayed vigorously growing RUBY tissues (Figure 3G-I). As
233 RUBY has been used as a visual selection marker in other plants (Yu *et al.*, 2023), we decided to
234 employ it as a visual selection marker during the early co-cultivation stage, eliminating the need
235 for a selection reagent.

236 ***Agrobacterium*-mediated *Cuscuta* transformation**

237 To conduct the *Agrobacterium*-mediated *Cuscuta* transformation, 4-day-old *C. campestris*
238 seedlings were chopped and infected by *A. tumefaciens* EHA105-*35S:RUBY*. *Agrobacterium*
239 infected segments were incubated on the co-cultivation media without growth hormones for five
240 days (Figure 4A). Subsequently, *Cuscuta* segments expressing RUBY were transferred to CIM
241 media (Figure 4B). The explants were cultured in CIM media for at least 8 weeks before being
242 transferred to shoot induction media (Figure 4C). Larger and darker red calli were obtained after
243 another 8 weeks of incubation on the shoot induction media (Figure 4D) and then transferred to
244 shoot elongation media when the red calli reached a size of 1 cm (Figure 4E). Calli grown on the
245 shoot elongation media started to produce shoots in two weeks (Figure 4F).

246 During the callus induction stage, the number of visible red spots on *A. tumefaciens*
247 EHA105-*35S:RUBY* infected *Cuscuta* segments were counted on 5, 15, 25, 35, and 45 days after
248 infection to track the transformation efficiency. Since we selected *Cuscuta* segments expressing
249 RUBY to callus induction media after 5-day co-cultivation, transformed calli represented 100%
250 on the fifth day of inoculation. The number of transformed calli slowly declined to 93.2%,
251 86.0%, 76.7 %, and 62.1% on the 15, 25, 35, and 45 days after inoculation, respectively (Figure
252 5A and Supp table 8).

253 Further declines in the number of stably transformed calli occurred over subsequent growth
254 stages. Percentages of RUBY callus growing on shoot elongation media, callus producing RUBY

255 *Cuscuta* shoots, and RUBY *Cuscuta* shoots coiled on host were 16%, 5.3%, and 2.8%,
256 respectively (Figure 5B and Supp table 9).

257 **Successful parasitism of transgenic RUBY *Cuscuta***

258 Once the RUBY *Cuscuta* shoots reached a size of 3 cm on the shoot elongation media, calli
259 with RUBY *Cuscuta* shoots were moved to magenta boxes containing the shoot elongation
260 media (Figure 6A). To observe the characteristic wrapping behavior of *Cuscuta*, a toothpick was
261 inserted into the media to serve as a substitute host. Within a day of introducing the toothpick,
262 RUBY *Cuscuta* coiled (Figure 6B) and produced haustoria (Figure 6C). We also introduced
263 RUBY *Cuscuta* stems to live host plants. Within 24 hours post-inoculation, the RUBY *Cuscuta*
264 stems exhibited coiling and initiated haustoria development on 1-week-old tomato (Figure 6D).
265 All host plants, both tomatoes (Figure 6E) and *Arabidopsis* (Figure 6F), were also successfully
266 parasitized by the RUBY *Cuscuta*. Approximately 2 months after transfer to beet hosts, RUBY
267 *Cuscuta* produced flowers (Figure 6G-H) and seeds (Figure 6I).

268 **Event-specific detections of transgenic lines**

269 From 8 attempts of the *Agrobacterium*-mediated *Cuscuta* transformation, 11 transgenic
270 events were generated (Supp table 9). To validate the T-DNA insertions, gDNA was extracted
271 from 2 well-developed transgenic events. Subsequently, TAIL-PCRs using right border (RB)
272 primers located in the 35S promoter of the *35S:RUBY* were conducted (Figure 7A). After
273 sequencing the amplicons, results showed that both transgenes lacked the RB sequences (gray
274 box, Figure 7A). Furthermore, the transgene of the first event contained a complete 35S
275 promoter, whereas the transgene from the second event had a truncated 35S promoter (Figure 7B
276 and Supp figure 1). By aligning TAIL-PCR sequences with *C. campestris* genome data, the
277 integration locations of transgenes were located on *C. campestris* Scaffold 32B and *C.*
278 *campestris* Scaffold 104, indicating that those events were independent transgenic plants (Figure
279 7B).

280 **Diffused RUBY pigments in host stems**

281 To compare the structural differences of haustoria between WT and transgenic RUBY
282 *Cuscuta*, WT *Cuscuta* and RUBY *Cuscuta* stems were inoculated on 2-week-old tomato
283 seedlings. The haustoria of wild-type *C. campestris* exhibited the typical hypersensitive response
284 near the epidermis without any visible color on the host stem (Figure 8A and E). When RUBY
285 *Cuscuta* was successfully coiled on the host stem but failed to penetrate, the red pigment was not

286 detected in host stems or vascular bundles (Figure 8B, F). Similarly, no RUBY pigment was
287 observed in the host stem during the early haustorium penetration stage of RUBY *Cuscuta*
288 (Figure 8C, G). However, we observed diffuse RUBY pigments (Figure 8D and white circles of
289 Figure 8H) in the area where successful haustoria development occurred, along with developed
290 searching hyphae (black arrows, Figure 8H).

291 The RUBY diffusion was also observed when RUBY *Cuscuta* was inoculated on *Arabidopsis*
292 Col-0 plants. After staining tissues with toluidine blue, we found that RUBY pigments were
293 mainly detected on cortex and phloem of host *Arabidopsis* stem (Figures 8I-K). RUBY was even
294 detected in regions away from *Cuscuta* haustoria (white circles of Figure 8I, L). Besides the
295 RUBY diffusion, there was no obvious physical difference between WT *Cuscuta* and RUBY
296 *Cuscuta* haustoria.

297 **Enhanced transformation efficiency using *CcGRF/GIF Cuscuta***

298 Since morphogenic genes have enhanced plant transformation efficiency (Lowe *et al.*, 2016;
299 Chen *et al.*, 2022), we tested whether *C. campestris WUS2* or *C. campestris GRF/GIF* can
300 promote transformation efficiency. Four-day-old *C. campestris* seedlings (Figure 9A) were
301 chopped and infected by EHA105 with *GUS*, *CcWUS2-GUS,* and *CcGRF/GIF-GUS* (Figure 9B).
302 After the co-cultivation, 50 infected meristem-containing-segments were placed on CIM media
303 (Figure 9C). Around 35-day-old *Cuscuta* segments infected by EHA105 with *GUS*, *CcWUS2-*
304 *GUS,* and *CcGRF/GIF-GUS* were harvested and stained (Figure 9D-F). More specifically,
305 segments expressing GUS were quantified and classified by sizes of the GUS expressing sectors,
306 such as no GUS, less than 0.2 mm GUS, between 0.2 to 2 mm GUS, and larger than 2 mm GUS,
307 aiming to distinguish the extent of GUS expression in a segment (Supp figure 2).

308 In terms of presence and absence of GUS expression, the transformation efficiencies using
309 *GUS*, *CcWUS2-GUS,* and *CcGRF/GIF-GUS* were 78.8%, 51.7%, and 74.8%, respectively
310 (Figure 10A). Notably, the transformation efficiency associated with *CcWUS2-GUS* was
311 significantly lower than *GUS* or *CcGRF/GIF-GUS.* In contrast, there was no significant
312 difference in transformation efficiency between GUS and *CcGRF/GIF-GUS*. Data from
313 categorized segments indicated that *Cuscuta* segments infected with *GUS* only showed a
314 significantly higher proportion in the below 0.2 mm category compared to *CcWUS2-GUS* and
315 *CcGRF/GIF-GUS* (Figure 10B). *Cuscuta* with *CcGRF/GIF-GUS* had a significantly higher
316 percentage in the over 2mm group than *GUS* only. These findings suggest that *GUS* only and

317 *CcGRF/GIF-GUS* had similar levels of transformation efficiency based on the presence or
318 absence of GUS expression. However, *CcGRF/GIF-GUS* significantly enhanced regeneration
319 efficiency during the callus induction stage, leading to more significant GUS expression
320 compared to *GUS* only.
321

322 **Discussion**

323 The lack of a protocol for transformation and regeneration of *Cuscuta* has hindered progress
324 in studying parasite gene functions and the mechanisms of *Cuscuta*-host interactions. Despite
325 previous studies demonstrating transformation of *Cuscuta* tissues (Srivastava & Dwivedi, 2001;
326 Borsics *et al.*, 2002; Švubová & Blehová, 2013; Lachner *et al.*, 2020), none have succeeded in
327 regenerating stably transformed *Cuscuta* plants that can be used to study the full range of
328 parasite biology. Here we describe a method for the relatively fast and efficient stable
329 transformation of *C. campestris* plants that behave as normal parasites, producing haustoria,
330 flowers, and seeds (Figure 6). The process hinges on *A. tumefaciens*-mediated transformation
331 with appropriate media for inducing callus and shoots. We estimate that the process yields about
332 2.7% of transformed plants and takes about 5 months. While this transformation efficiency may
333 not be high compared to easily transformable plants like tobacco, it stands out as remarkably
334 successful for the initial attempt with a transformation recalcitrant species.

335 An important innovation was use of the recently developed RUBY reporter (He *et al.*, 2020).
336 RUBY encodes enzymes for synthesizing betalain from tyrosine and is useful for visually
337 monitoring transformation events without using fluorescence microscopy or a chemical selection
338 process. However, recent studies reported that RUBY may cause low regeneration efficiency and
339 poor fertility during seed development due to the lack of the essential amino acid tyrosine. For
340 example, maize expressing a strong RUBY reporter had growth retardation (Lee *et al.*, 2023).
341 While we are mindful that the RUBY reporter could be detrimental to *Cuscuta*, evidence to date
342 suggests that transgenic RUBY *Cuscuta* shows normal, though somewhat slower, growth
343 compared to non-transgenic plants. But importantly, the vivid RUBY reporter was a valuable
344 asset in the development of the protocol and may not be easily replaced by other selectable
345 markers.

346 The use of morphogenic genes appears to contribute positively to the *Cuscuta* transformation
347 protocol. We observed an enhancement in transformation efficiency with *Cuscuta GRF-GIF*, a
348 phenomenon similar to previously reported findings in wheat and citrus transformation
349 (Debernardi *et al.*, 2020). In *Agrobacterium*-mediated *Cuscuta* transformation, *CcGRF-GIF*
350 showed minimal impact on the overall presence/absence ratios of GUS transformation efficiency
351 (Figure 10A). However, the number of GUS segments larger than 2mm was significantly
352 increased in *CcGRF-GIF-GUS* infected *Cuscuta* compared to *Cuscuta* segments with *GUS* only

353 (Figure 10B). This suggests that *CcGRF-GIF* may not significantly influence *Agrobacterium*-
354 mediated transformation but could enhance the regeneration of transformed tissue, as previously
355 reported (Debernardi *et al.*, 2020). Further investigation is needed regarding the use of *CcGRF-*
356 *GIF* with *Cuscuta* transformation, as well as whether Ccu-miR396 can improve the efficiency of
357 stable transformation. In contrast, using *CcWUS-GUS* in transformations led to lower
358 presence/absence ratios of GUS transformation efficiency than *GUS* alone or *CcGRF-GIF-GUS*
359 (Figure 10A). We hypothesize that, similar to previous studies, the constitutive *CcWUS2*
360 expression by the 35S promoter may interfere with the *Cuscuta* development genes, resulting in
361 the decreased transformation efficiency (Rashid *et al.*, 2007; Lowe *et al.*, 2016; Hoerster *et al.*,
362 2020; Kadri *et al.*, 2021).

363 In this study we observed what appears to be movement of RUBY pigment from the
364 transformed parasite into host cells in the area around developed *Cuscuta* searching hyphae
365 inside vascular structures of the host stem (Figure 8H, K). However, the RUBY diffusion was
366 not observed during the early invasion stage (asterisk, Figure 8G). This is intriguing given the
367 ability of *Cuscuta* to exchange large numbers of mobile small RNAs, mRNAs and proteins
368 between *Cuscuta* and host plants. Here, toluidine staining suggest that RUBY pigments were
369 detected in host phloem and cortex (Figure 8K). Studies of long distance movement of mRNAs
370 suggest trafficking occurs in parasite and host phloem (Kim *et al.*, 2014; Park *et al.*, 2022), while
371 small RNAs appear to concentrate in haustorial regions (Shahid *et al.*, 2018). Consistent with
372 these findings, we detect the presence of RUBY pigment in both tissues, perhaps reflecting
373 general movement of molecules from parasite to host. It is interesting to note the differences in
374 patterns between the two host species, with a significant amount of RUBY found in the
375 *Arabidopsis* cortex, as compared to a distinct pattern around vascular bundles in tomato stems.
376 The existence of a partially effective defense in tomato may contribute to this. Thus, this
377 observation suggests that the RUBY reporter system serves not only as a selection marker for
378 transformation, but also as an indicator of events during parasitism at the molecular level.
379 Specifically, the RUBY movement prompts speculation about potential mechanisms of transfer:
380 1) translation of mobile RNA, wherein mRNAs of betalain synthesis enzymes move from
381 *Cuscuta* to the host stem and are translated near the haustoria; 2) mobile proteins from *Cuscuta*
382 to host, involving the export of three betalain synthesis enzymes from *Cuscuta* that produced
383 betalain in the host stem; or 3) the movement of betalain pigment itself from *Cuscuta* to the host.

384 Fortunately, we now have the tools to validate these hypotheses. It would be interesting to
385 generate transgenic *Cuscuta* expressing a fluorescence reporter gene fused with endoplasmic
386 reticulum (ER) targeting peptide, such as ER-YFP (Sager *et al.*, 2020), which produces a non-
387 mobile product. But regardless of the details, the ability to generate transgenic *Cuscuta* as
388 described here will enable many more experiments, and much greater understanding, of *Cuscuta*
389 biology.
390

391 **Acknowledgement**
392 This work was supported by the USDA-AFRI- 2023-67013-39896 to SP and JW, CAFNR-JOY,
393 University of Missouri to SP, Research Council, University of Missouri to SP and NSF award IOS-
394 1645027 to JW. We thank Duy Trinh who made the *CcGRF-GIF* construction. Grammarly generated
395 responses to the following AI prompts: Prompts created by Grammarly- "Improve it".
396

397 **Conflicting interests**
398 All authors declare that they have no conflicting interests**.**
399

400 **Author contributions**
401 SP, HL, and JW conceived the ideas and designed methodology. SA, AM, VB, HG, and SP conducted
402 lab-work and analyzed the data. SA, AM, SP, and JW led the writing of the manuscript. All authors
403 contributed critically to the drafts and gave final approval for publication.
404

405 **Data availability**
406 The datasets used and/or analyzed during the current study are available from the corresponding author
407 upon request.
408

409 **References**

410 **Bandaranayake PCG, Yoder JI. 2018.** Factors affecting the efficiency of Rhizobium rhizogenes root
411 transformation of the root parasitic plant Triphysaria versicolor and its host Arabidopsis thaliana.
412 *Plant Methods* **14**: 61.
413 **Bernal-Galeano V, Beard K, Westwood JH. 2022.** An artificial host system enables the obligate
414 parasite Cuscuta campestris to grow and reproduce in vitro. *Plant Physiology* **189**(2): 687-702.
415 **Borsics T, Mihálka V, Oreifig AS, Bárány I, Lados M, Nagy I, Jenes B, Toldi O. 2002.** Methods for
416 genetic transformation of the parasitic weed dodder (*Cuscuta trifolii* Bab. et Gibs) and for PCR-
417 based detection of early transformation events. *Plant Science* **162**(2): 193-199.
418 **Bull T, Debernardi J, Reeves M, Hill T, Bertier L, Van Deynze A, Michelmore R. 2023.** GRF–GIF
419 chimeric proteins enhance in vitro regeneration and Agrobacterium-mediated transformation
420 efficiencies of lettuce (Lactuca spp.). *Plant Cell Reports* **42**(3): 629-643.
421 **Chen Z, Debernardi JM, Dubcovsky J, Gallavotti A. 2022.** Recent advances in crop transformation
422 technologies. *Nature Plants* **8**(12): 1343-1351.
423 **Cudney DW, Orloff SB, Reints JS. 1992.** An Integrated Weed Management Procedure for the Control
424 of Dodder (Cuscuta indecora) in Alfalfa (Medicago sativa). *Weed Technology* **6**(3): 603-606.
425 **Dawson JH, Musselman LJ, Wolswinkel P, Dörr I. 1994.** Biology and control of Cuscuta. *Reviews of*
426 *Weed Science* **6**: 265-317.
427 **Debernardi JM, Tricoli DM, Ercoli MF, Hayta S, Ronald P, Palatnik JF, Dubcovsky J. 2020.** A
428 GRF–GIF chimeric protein improves the regeneration efficiency of transgenic plants. *Nature*
429 *Biotechnology* **38**(11): 1274-1279.
430 **Dechassa N, Regassa B. 2021.** Current Status, Economic importance and Management of Dodders
431 (Cuscuta Spp) of Important Crops.
432 **Feng Q, Xiao L, He Y, Liu M, Wang J, Tian S, Zhang X, Yuan L. 2021.** Highly efficient, genotype-
433 independent transformation and gene editing in watermelon (Citrullus lanatus) using a chimeric
434 ClGRF4-GIF1 gene. *J Integr Plant Biol* **63**(12): 2038-2042.
435 **Fernández-Aparicio M, Rubiales D, Bandaranayake PC, Yoder JI, Westwood JH. 2011.**
436 Transformation and regeneration of the holoparasitic plant Phelipanche aegyptiaca. *Plant*
437 *Methods* **7**(1): 36.
438 **Galloway AF, Knox P, Krause K. 2020.** Sticky mucilages and exudates of plants: putative
439 microenvironmental design elements with biotechnological value. *New Phytologist* **225**(4): 1461-
440 1469.
441 **Goldwasser Y, Sazo MRM, Lanini WT. 2012.** Control of Field Dodder (Cuscuta campestris)
442 Parasitizing Tomato with ALS-Inhibiting Herbicides. *Weed Technology* **26**(4): 740-746.
443 **He Y, Zhang T, Sun H, Zhan H, Zhao Y. 2020.** A reporter for noninvasively monitoring gene
444 expression and plant transformation. *Horticulture Research* **7**(1): 152-152.
445 **Hegenauer V, Fürst U, Kaiser B, Smoker M, Zipfel C, Felix G, Stahl M, Albert M. 2016.** Detection
446 of the plant parasite Cuscuta reflexa by a tomato cell surface receptor. *Science* **353**(6298): 478-
447 481.
448 **Hegenauer V, Slaby P, Körner M, Bruckmüller J-A, Burggraf R, Albert I, Kaiser B, Löffelhardt B,**
449 **Droste-Borel I, Sklenar J. 2020.** The tomato receptor CuRe1 senses a cell wall protein to
450 identify Cuscuta as a pathogen. *Nature communications* **11**(1): 5299.
451 **Hoerster G, Wang N, Ryan L, Wu E, Anand A, McBride K, Lowe K, Jones T, Gordon-Kamm B.**
452 **2020.** Use of non-integrating Zm-Wus2 vectors to enhance maize transformation: non-integrating
453 WUS2 enhances transformation. *In Vitro Cellular & Developmental Biology-Plant* **56**(3): 265-
454 279.
455 **Ishida JK, Yoshida S, Ito M, Namba S, Shirasu K. 2011.** Agrobacterium rhizogenes-Mediated
456 Transformation of the Parasitic Plant Phtheirospermum japonicum. *PLoS ONE* **6**(10): e25802.

457 **Johnsen HR, Striberny B, Olsen S, Vidal-Melgosa S, Fangel JU, Willats WGT, Rose JKC, Krause**
458 **K. 2015.** Cell wall composition profiling of parasitic giant dodder (Cuscuta reflexa) and its hosts:
459 a priori differences and induced changes. *New Phytologist* **207**(3): 805-816.
460 **Kadri A, Grenier De March G, Guerineau F, Cosson V, Ratet P. 2021.** WUSCHEL Overexpression
461 Promotes Callogenesis and Somatic Embryogenesis in Medicago truncatula Gaertn. *Plants*
462 *(Basel)* **10**(4).
463 **Kaiser B, Vogg G, Fürst UB, Albert M. 2015.** Parasitic plants of the genus Cuscuta and their interaction
464 with susceptible and resistant host plants. *Frontiers in Plant Science* **6**.
465 **Kim G, LeBlanc ML, Wafula EK, dePamphilis CW, Westwood JH. 2014.** Genomic-scale exchange of
466 mRNA between a parasitic plant and its hosts. *Science* **345**(6198): 808-811.
467 **Lachner LA-M, Galstyan L, Krause K. 2020.** A highly efficient protocol for transforming Cuscuta
468 reflexa based on artificially induced infection sites. *Plant Direct* **4**(8): e00254.
469 **Lanini W, Kogan M. 2005.** Biology and management of Cuscuta in crops. *International Journal of*
470 *Agriculture and Natural Resources* **32**(3): 127-141.
471 **Lee K, Kang M, Ji Q, Grosic S, Wang K. 2023.** New T-DNA binary vectors with NptII selection and
472 RUBY reporter for efficient maize transformation and targeted mutagenesis. *Plant Physiology*
473 **192**(4): 2598-2603.
474 **Lee K, Wang K. 2023.** Strategies for genotype-flexible plant transformation. *Current Opinion in*
475 *Biotechnology* **79**: 102848.
476 **Liu N, Shen G, Xu Y, Liu H, Zhang J, Li S, Li J, Zhang C, Qi J, Wang L, Wu J. 2020.** Extensive
477 Inter-plant Protein Transfer between Cuscuta Parasites and Their Host Plants. *Mol Plant* **13**(4):
478 573-585.
479 **Lowe K, Wu E, Wang N, Hoerster G, Hastings C, Cho MJ, Scelonge C, Lenderts B, Chamberlin M,**
480 **Cushatt J, et al. 2016.** Morphogenic Regulators Baby boom and Wuschel Improve Monocot
481 Transformation. *Plant Cell* **28**(9): 1998-2015.
482 **Nagar R, Singh M, Sanwal GG. 1984.** Cell Wall Degrading Enzymes in Cuscuta reflexa and Its Hosts.
483 *Journal of Experimental Botany* **35**(8): 1104-1112.
484 **Park SY, Shimizu K, Brown J, Aoki K, Westwood JH. 2022.** Mobile Host mRNAs Are Translated to
485 Protein in the Associated Parasitic Plant Cuscuta campestris. *Plants (Basel)* **11**(1).
486 **Pradhan Mitra P, Loqué D. 2014.** Histochemical staining of Arabidopsis thaliana secondary cell wall
487 elements. *J Vis Exp*(87).
488 **Rashid SZ, Yamaji N, Kyo M. 2007.** Shoot formation from root tip region: a developmental alteration
489 by WUS in transgenic tobacco. *Plant Cell Reports* **26**(9): 1449-1455.
490 **Runyon JB, Mescher MC, De Moraes CM. 2006.** Volatile chemical cues guide host location and host
491 selection by parasitic plants. *Science* **313**(5795): 1964-1967.
492 **Sager R, Wang X, Hill K, Yoo B-C, Caplan J, Nedo A, Tran T, Bennett MJ, Lee J-Y. 2020.** Auxin-
493 dependent control of a plasmodesmal regulator creates a negative feedback loop modulating
494 lateral root emergence. *Nature Communications* **11**(1): 364.
495 **Shahid S, Kim G, Johnson NR, Wafula E, Wang F, Coruh C, Bernal-Galeano V, Phifer T,**
496 **dePamphilis CW, Westwood JH, Axtell MJ. 2018.** MicroRNAs from the parasitic plant
497 Cuscuta campestris target host messenger RNAs. *Nature* **553**: 82.
498 **Srivastava S, Dwivedi UN. 2001.** Plant regeneration from callus of Cuscuta reflexa–an angiospermic
499 parasite–and modulation of catalase and peroxidase activity by salicylic acid and naphthalene
500 acetic acid. *Plant Physiology and Biochemistry* **39**(6): 529-538.
501 **Švubová R, Blehová A. 2013.** Stable transformation and actin visualization in callus cultures of dodder
502 (Cuscuta europaea). *Biologia* **68**(4): 633-640.
503 **Tomilov A, Tomilova N, Yoder JI. 2007.** Agrobacterium tumefaciens and Agrobacterium rhizogenes
504 transformed roots of the parasitic plant Triphysaria versicolor retain parasitic competence. *Planta*
505 **225**(5): 1059-1071.
506 **Vaughn KC. 2002.** Attachment of the parasitic weed dodder to the host. *Protoplasma* **219**(3): 227-237.

Yu J, Deng S, Huang H, Mo J, Xu Z-F, Wang Y. 2023. Exploring the Potential Applications of the Noninvasive Reporter Gene RUBY in Plant Genetic Transformation. *Forests* **14**(3): 637.

Zuo J, Niu Q-W, Frugis G, Chua N-H. 2002. The WUSCHEL gene promotes vegetative-to-embryonic transition in Arabidopsis. *The Plant Journal* **30**(3): 349-359.

512 **Figure 1.** Process of *Agrobacterium*-mediated *Cuscuta* transformation using *35S:GUS-pMAS:GFP*
513 construct. *Cuscuta* seedlings (A) were cut by scissors (B) and dipped in liquid MMS containing *A.*
514 *tumefaciens* EHA105-*35S:GUS-pMAS:GFP* (C). An excessive *Agrobacteria* was cultivated from
515 infected tissue five days after inoculation on the co-cultivation media (D). Explants were incubated on
516 CIM (E). An explant imaged under blue excitation light (F), yellow excitation light (G), and bright
517 field (H). Images from F-H were merged (I).
518
519 **Figure 2.** Effect of cytokinins and auxin on GFP positive calli formation after inoculation with
520 *Agrobacterium tumefaciens* EHA105 containing *35S:GUS-pMAS:GFP*. Different types and
521 concentrations of cytokinins (BAP and TDZ) and auxin (NAA) were tested (n=10). Six independent
522 biological replicates were performed. Data are presented as the mean ± standard deviation. Groups with
523 different letters vary significantly (two-way ANOVA-Tukey test, P,0.05).
524 **Figure 3.** RUBY expression in explants. RUBY expression in cut explants (A, B, C) and bulk chopped
525 explants (D, E, F) 40 days after inoculation. Callus expressing RUBY developed in bulk chopped
526 explants 4 months after inoculation (G, H, I).
527
528 **Figure 4**. Process of *Agrobacterium*-mediated *Cuscuta* transformation using *35S:RUBY* construct.
529 *Cuscuta* seedlings were infected by EHA105-*35S:RUBY* and incubated on co-cultivation media for 5
530 days (A) and separated on CIM (B). RUBY-expressing calli were grown on CIM (C) and SIM (D). Calli
531 expressing RUBY were selected and transferred to SEM (E) and produced shoots (F).
532
533 **Figure 5**. *C. campestris* transformation efficiency with the RUBY reporter gene. (A) Transformation rate
534 on various days following inoculation. Sixteen independent replicates were performed (n=50). (B) The
535 callus induction rate, shoot induction rate, and coiling rate were measured for RUBY *Cuscuta*. Eight
536 independent replicates were performed (n=50). Data are presented as the mean ± standard deviation.
537
538 **Figure 6**. Transgenic RUBY *Cuscuta* attaching to non-living and living hosts. A shoot from transgenic
539 callus (A) coiled on a toothpick (B-C). (C) Zoomed-in image of the black box in (B) showing haustoria
540 formation. RUBY *Cuscuta* coiled on (D) and parasitizing (E) the stem of a 2-week-old tomato. (F) RUBY
541 *Cuscuta* was successfully grown on *Arabidopsis*. (I) Transgenic RUBY *Cuscuta* produced flowers on
542 beets (G-H) and seeds.
543

544 **Figure 7.** Alignment of sequences from TAIL PCRs and the *35S:RUBY* construct. (A) Diagram of 35S
545 promoter and RUBY near RB region in *35S:RUBY*. Red arrow, yellow arrow, and gray box are RUBY,
546 35S promoter, and right border, respectively. Black arrows (RB1 and RB2) are primers used for the TAIL
547 PCRs. (B) Schematic designs of T-DNA sequences and insertion points into the *C. campestris* genome.
548 Yellow boxes indicate 35S promoter of *35S:RUBY* and white boxes are *C. campestris* genome sequences.
549
550 **Figure 8.** Cross sections of *Cuscuta* haustoria on tomato or *Arabidopsis* stems. Haustoria of WT *C.*
551 *campestris* successfully penetrated tomato stems and established a connection with the host vascular
552 bundle (A, E). RUBY *Cuscuta* coiling around a host tomato stem but failing to penetrate (B, F). RUBY
553 *Cuscuta* successfully attaching to tomato is shown at early (C, G) and mature (D, H) haustoria
554 development stages. (E-H): Zoomed-in images of the white box region of corresponding images in (A-D).
555 RUBY *Cuscuta* penetrated and developed haustoria on *Arabidopsis* Col-0 stem (I). Images of the white
556 box in (I) before staining (J) and after toluidine staining (K). Vertical section of *Cuscuta* haustorium on
557 *Arabidopsis* Col-0 (L). Asterisks (*), white circles, and black arrows indicate the presence of *Cuscuta*
558 haustorium, area of diffused RUBY pigment, and searching hyphae, respectively. xy, xylem; ixf, xylem
559 fibres; ph, phloem; cor, cortex.
560
561 **Figure 9**. *Agrobacterium*-mediated *Cuscuta* transformation using chopped seedlings. Four-day-old
562 seedlings (A) were chopped (B) and inoculated with *Agrobacterium tumefaciens* strain EHA105
563 harboring *35S:GUS-pMAS:GFP*. (C) Infected segments were incubated on cocultivation media. (D-F)
564 Approximately 35 days after inoculation, segments infected by *35S:GUS-pMAS:GFP, 35S:CcWUS2-GUS*
565 and *35S: CcGRF-CcGIF-GUS* were stained with X-gluc solution.
566
567 **Figure 10.** Effect of *CcWUS2* and *CcGRF/GIF* on *Agrobacterium*-mediated *Cuscuta* transformation. (A)
568 The transformation efficiencies of *GUS* (blue bar), *CcWUS2-GUS* (purple bar), and *CcGRF/GIF-GUS*
569 (pink bar) were compared. (B) GUS expressions were classified into four groups according to the size of
570 GUS expression. Thirty independent replicates were performed (n=50). Data are presented as the mean ±
571 standard deviation.
572
573 **Supplementary Figure 1.** Results of TAIL-PCRs to confirm genomic integration. Sequences are details
574 of the diagram in Figure 8B. The *35S:RUBY* vector sequences (yellow highlights) are linked to *C.*
575 *campestris* genome scaffolds 32B and 104.
576

577 **Supplementary Figure 2.** Various sizes of GUS expression sectors in transformed tissues. Following the
578 GUS staining assay, the segments were classified into four groups: No GUS (A-C), less than 0.2 mm
579 GUS (D-F), between 0.2 to 2 mm GUS (G-I), and larger than 2 mm GUS (J-L). The bars represent a scale
580 of 500 μm.

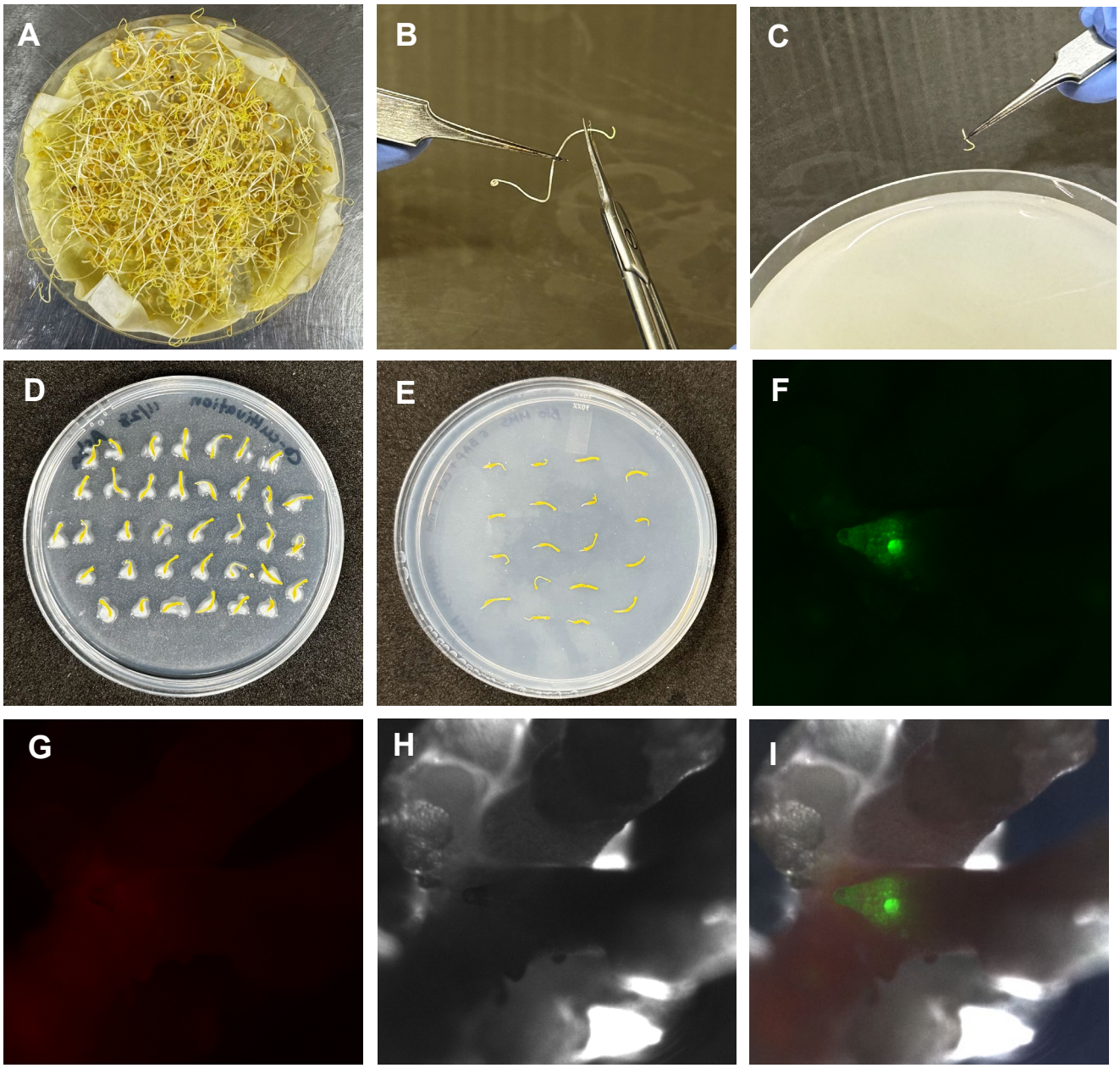

Figure 1

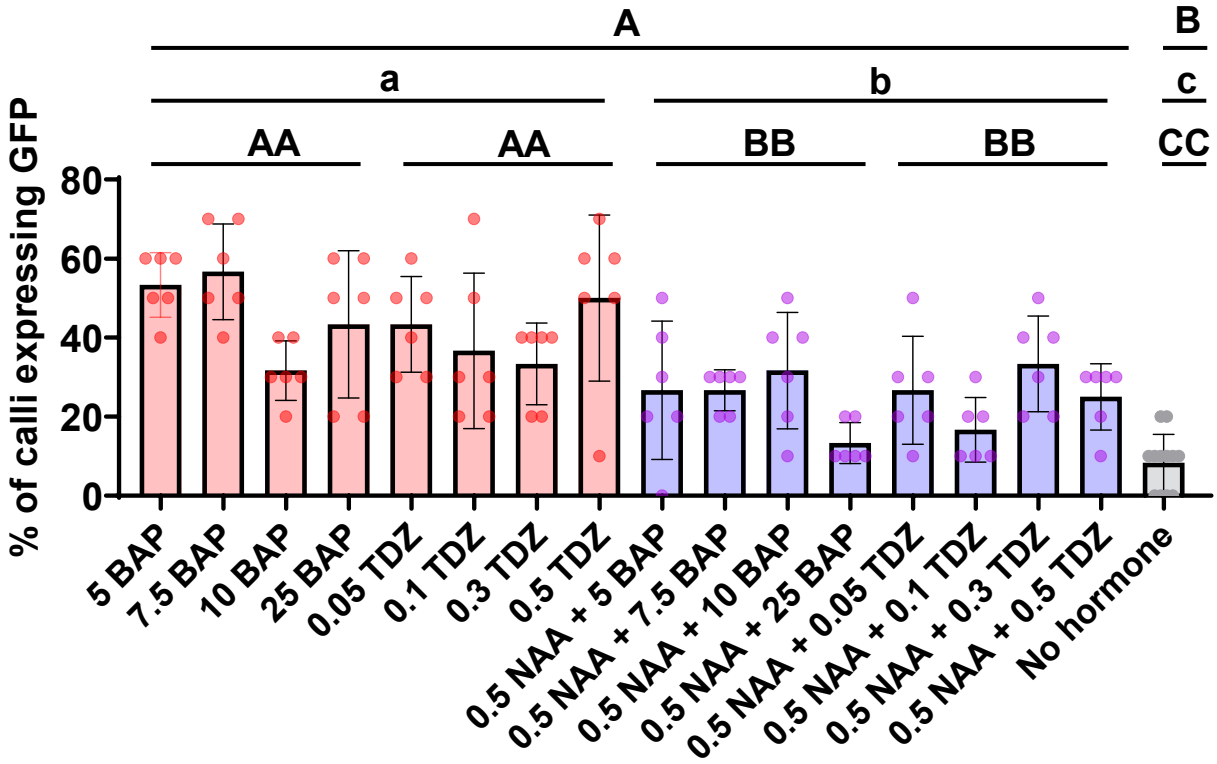
A
B
a
b
c
AA
AA
BB
BB
CC
% of calli expressing GFP
80
60
40
20
0
5 BAP
7.5 BAP
10 BAP
25 BAP
0.05 TDZ
0.1 TDZ
0.3 TDZ
0.5 TDZ
0.5 NAA + 5 BAP
0.5 NAA + 7.5 BAP
0.5 NAA + 10 BAP
0.5 NAA + 25 BAP
0.5 NAA + 0.05 TDZ
0.5 NAA + 0.1 TDZ
0.5 NAA + 0.3 TDZ
0.5 NAA + 0.5 TDZ
No hormone

Figure 2

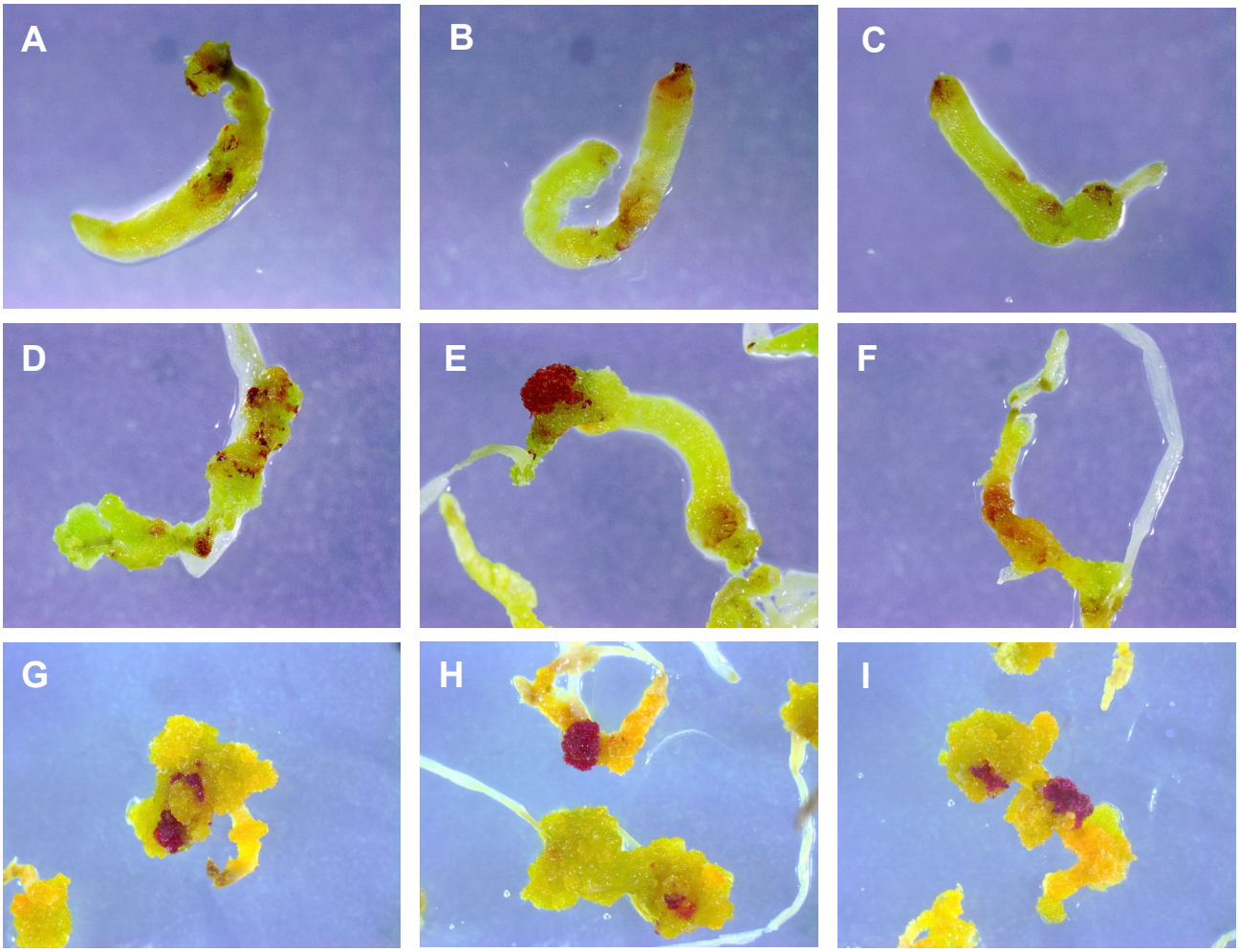

Figure 3

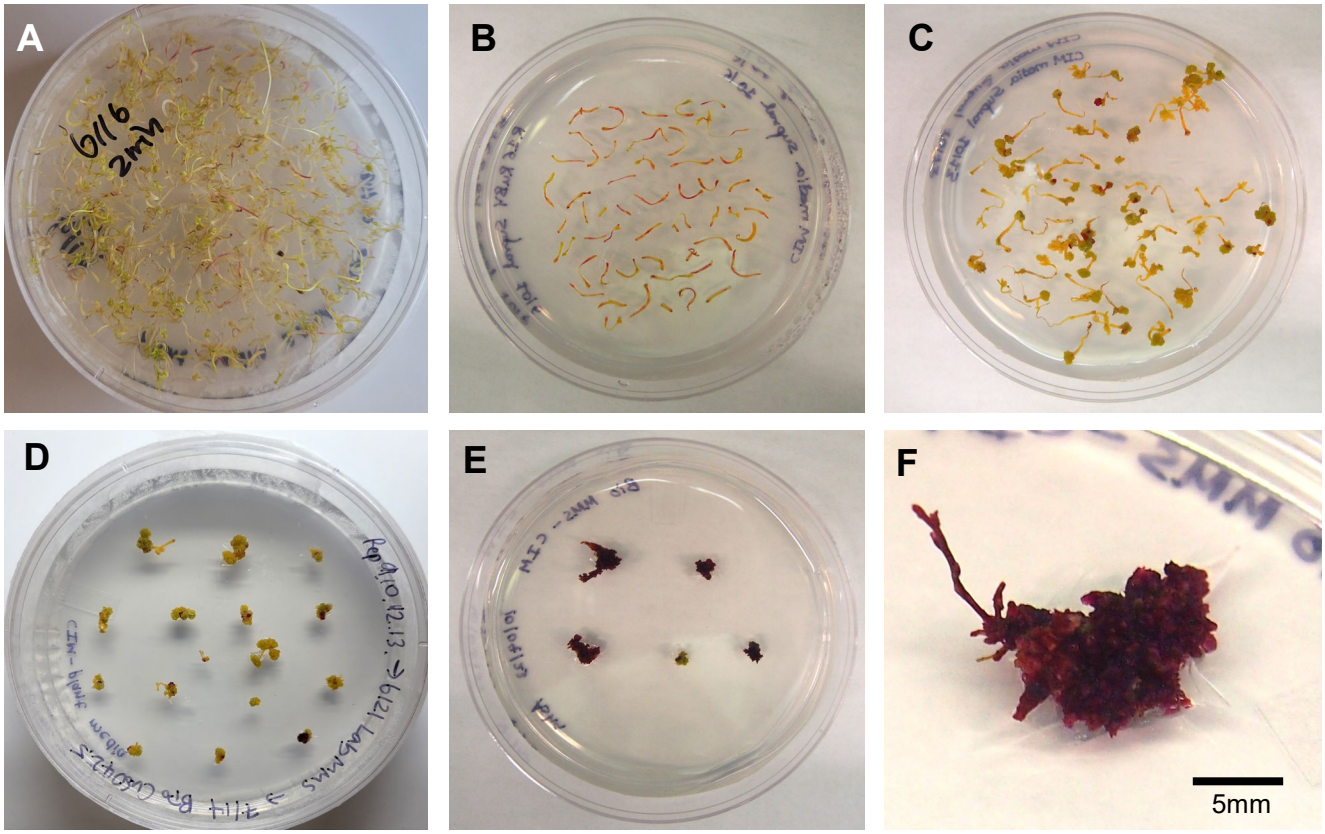

Figure 4

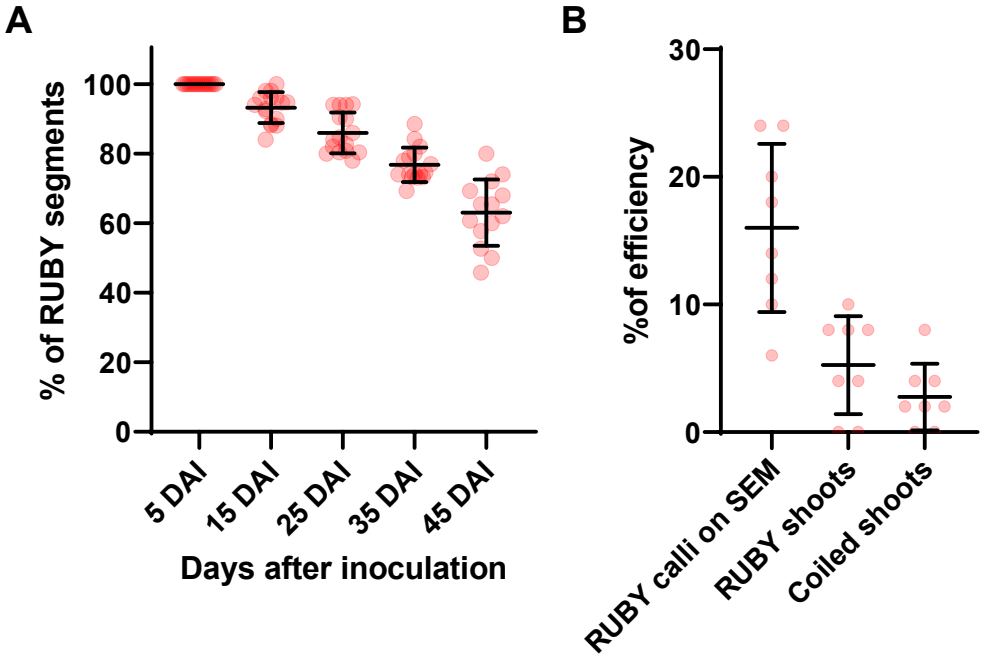
A
% of RUBY segments
100
80
60
40
20
0
5 DAI
15 DAI
25 DAI
35 DAI
45 DAI
Days after inoculation
B
%of efficiency
30
20
10
0
RUBY calli on SEM
RUBY shoots
Coiled shoots

Figure 5

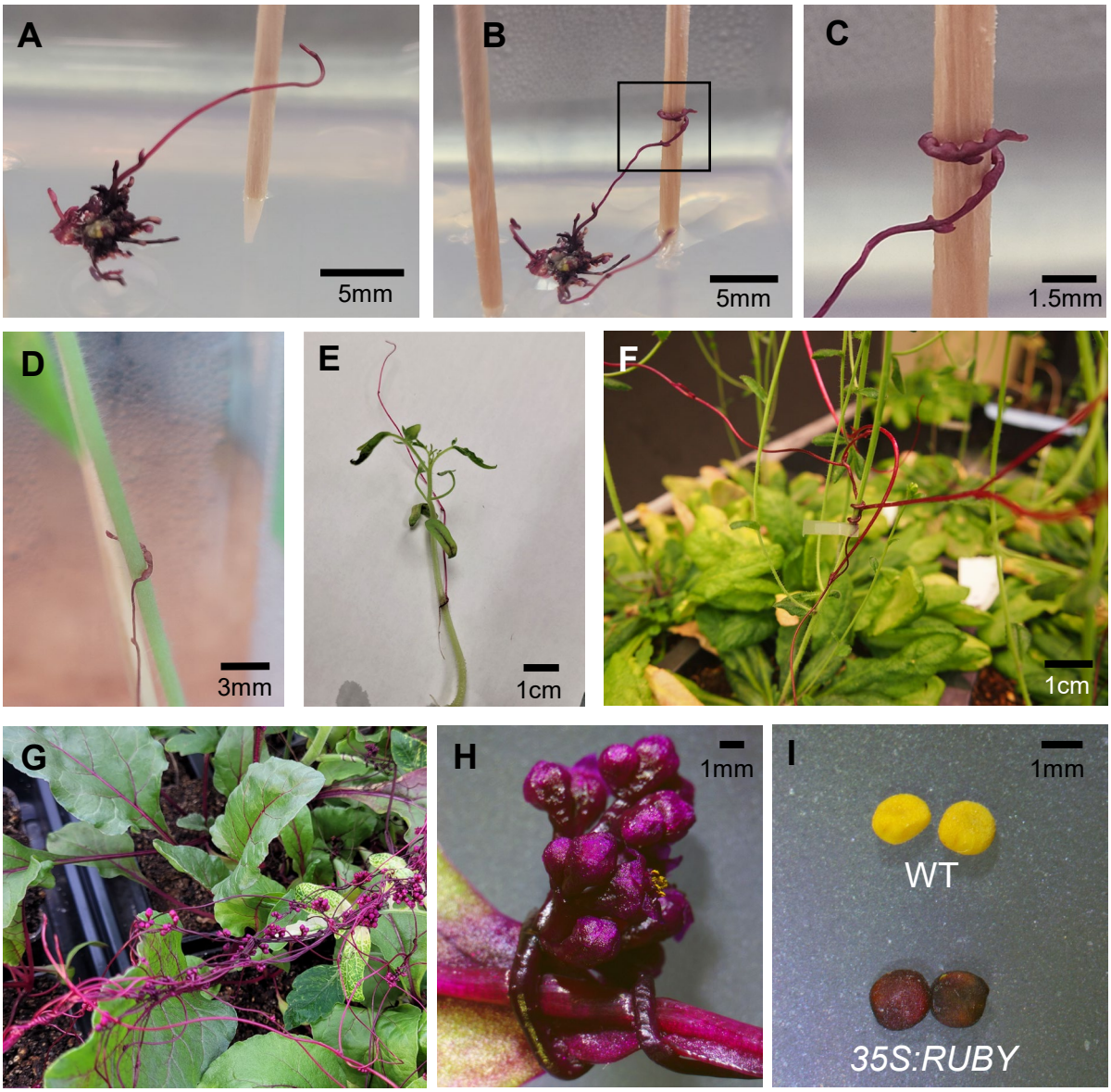

Figure 6

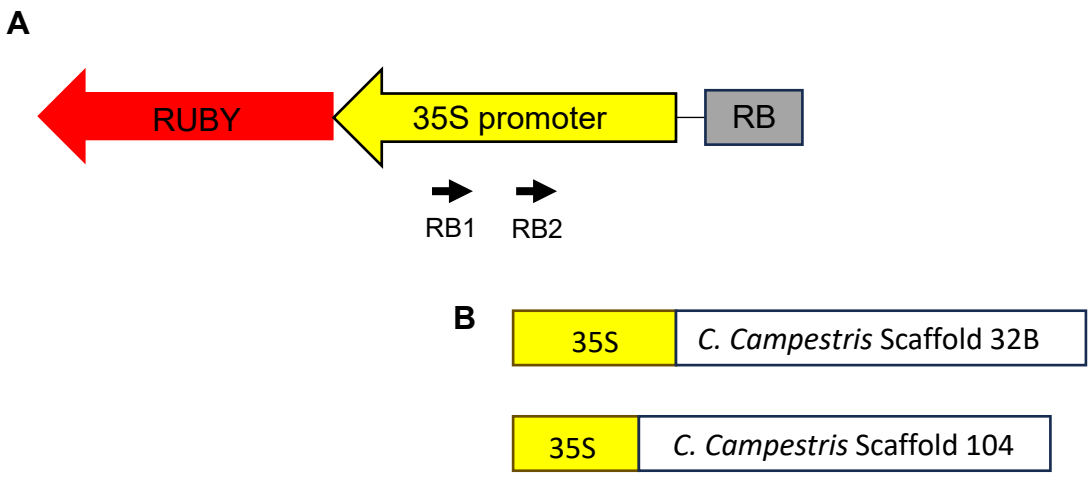
A
RUBY
35S promoter
RB
RB1
RB2
B
35S
C. Campestris Scaffold 32B
35S
C. Campestris Scaffold 104

Figure 7

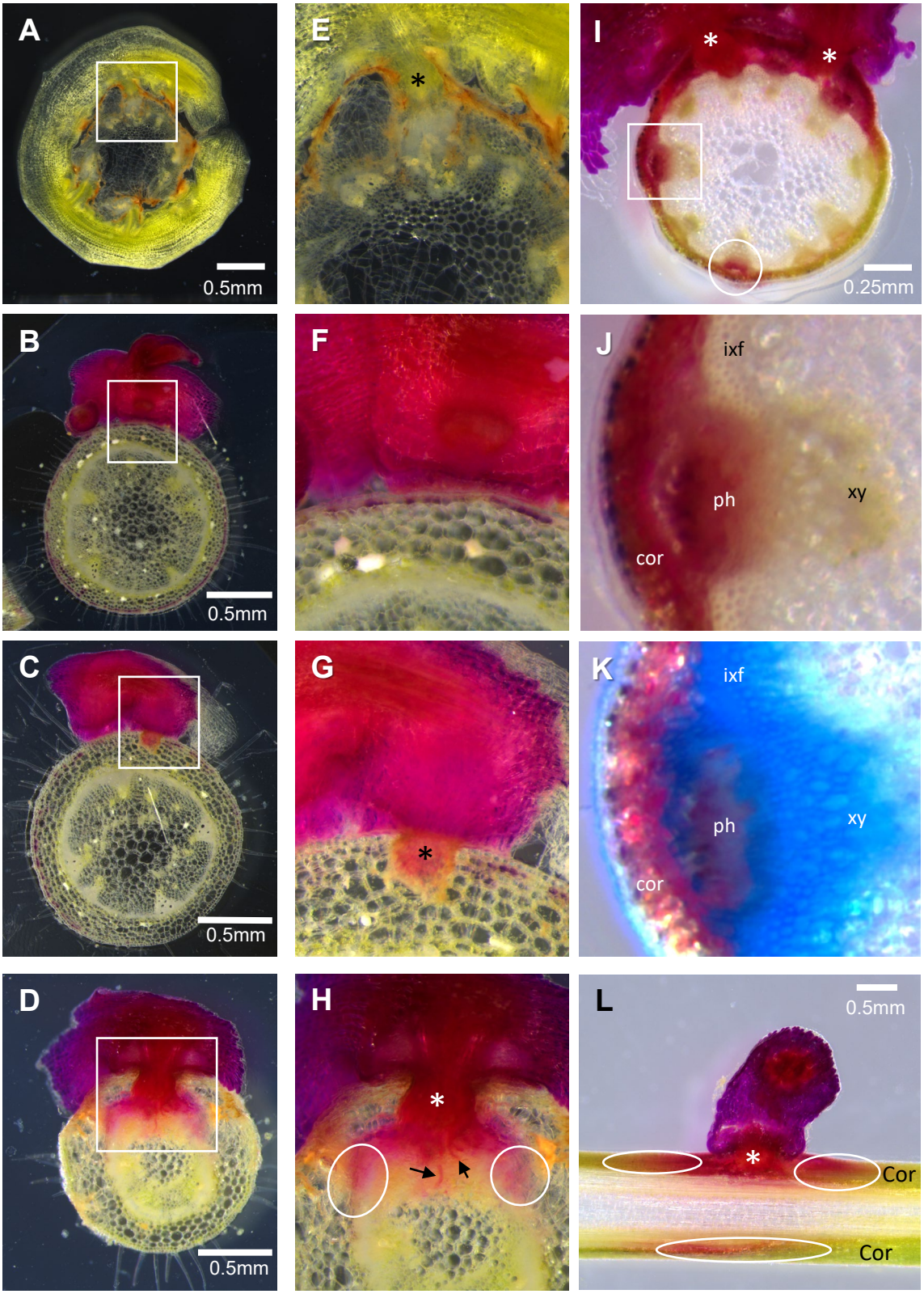
A
0.5mm
E
*
I
*
*
0.25mm
B
0.5mm
F
J
ixf
ph
xy
cor
C
0.5mm
G
*
K
ixf
ph
xy
cor
D
0.5mm
H
*
L
0.5mm
*
Cor
Cor

Figure 8

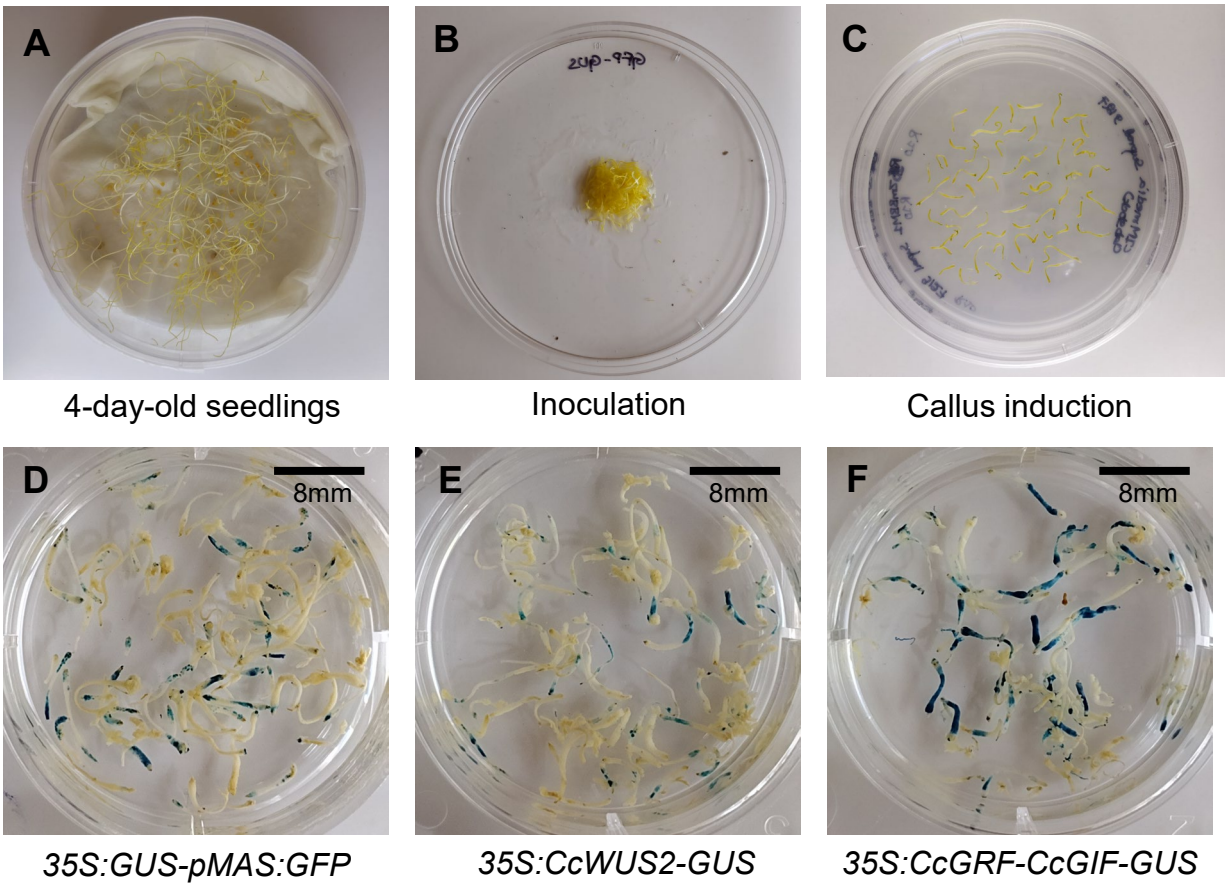
A
B
C
4-day-old seedlings
Inoculation
Callus induction
D
8mm
E
8mm
F
8mm
35S:GUS-pMAS:GFP
35S:CcWUS2-GUS
35S:CcGRF-CcGIF-GUS

Figure 9

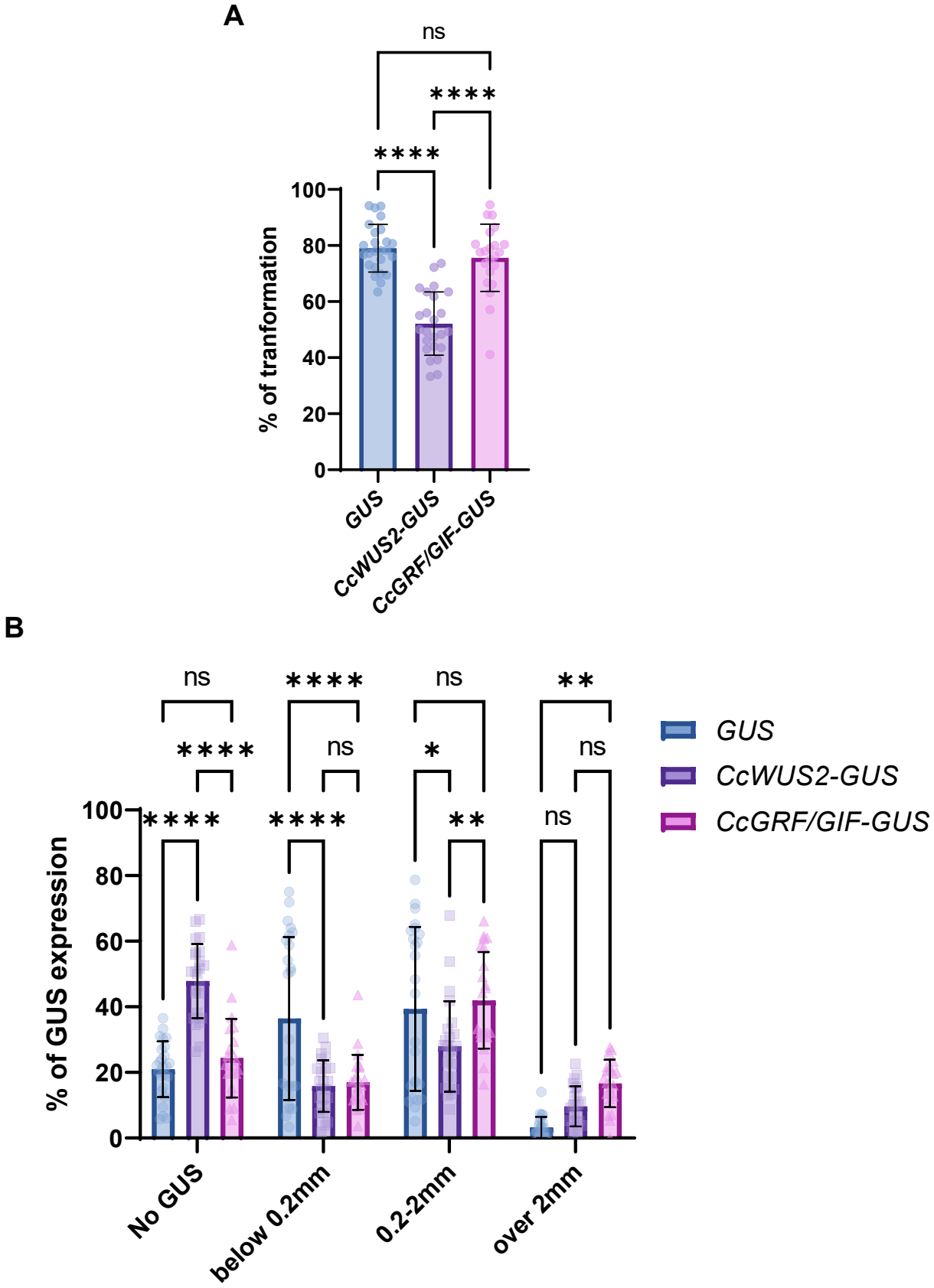
A
ns
****
****
100
80
60
40
20
0
% of tranformation
GUS
CcWUS2-GUS
CcGRF/GIF-GUS
B
ns
****
ns
**
****
ns
*
ns
****
****
**
ns
100
80
60
40
20
0
% of GUS expression
No GUS
below 0.2mm
0.2-2mm
over 2mm
GUS
CcWUS2-GUS
CcGRF/GIF-GUS

Figure 10

35S promoter and scaffolds 32B

ATGCTCCTCGTGGGTGGGGGTCCATCTTTGGGACCACTGTCGGCAGAGGCATCTTGAAC
GATAGCCTTTCCTTTATCGCAATGATGGCATTTGTAGGTGCCACCTTCCTTTTCTACTGTCC
TTTTGATGAAGTGACAGATAGCTGGGCAATGGAATCCGAGGAGGTTTCCCGATATTACCCT
TTGTAGAAAAGTCTCAAATCATCCATATATTCGATTGATTCTTTGCAGTACCCTTACCCGAC
TTATGGTGATACTTTATCTTCTAAAGGATTTCATATTCTCAGTGAGAATATGAAACGATCCA
AACGTACGAGACTTCCGACAACTTCTATGGATGTTATTTCACATTATCATCCTACAACAATT
CAAGTTGATAGCATTCCAATCGATCGCCAAATCTCTATCGGGTCAATCAACTAGCCCTTTG
ATCGCCTTCTTATTGGCCCTATCTGGGTGGACCCCTTCTGACCAGTCGTTCATCCCTCCGT
GGCGCGGCACACTTGTCCTACCGTCACCGAGTCAAGTCCCAAGCTGGTTAGCCATGGGTT
TACACCCATCACTTGGTACCCAATCTGGTGTGATTATTTGATATTGTTCTTATTTTTGTACTC
CCTACATCCTATTAGGACTTTCCAAATTCAAAGAAAAAATGTGTTGTCTATTATTTTTTCTCA
ATAATGAAATTTAATCACACTCTTC

35S promoter and scaffolds 104

ATGCTCCTCGTGGGTGGGGGTCCATCTTTGGGACCACTGTCGGCAGAGGCATCTTGGAC
GATAGCCTTTCCTTTATCGCAATGATGGCATTTGTAGGTGCCACCTTCCTTTTCTACTGTCC
TTTTGATGAAGTGACAGATAGCTGGGCAATGGAATCCGAGGAGGTTTCCCGATATTACCCT
ATCCATGAAACTTAGGAGTTCGCACCCCGCAGTTTCGTCCACCATTTGATCTGGACTGGG
GAGGGGGTATGAATCCATTGGACAAGCCTTGTTCAAGTCCGTATAATCCACACACATTCTC
CACGTGTCGCCCTTGGGAGCAAGGACAACGTTGGCCAGCCAATCCGGGTACTTGACTTC
CCGGATGTGACCAACACTGAGGAGGTCTCTCACTTCCTTCTTGACGAAGTCTCGCCGGTC
ACTCGCCAGGTACCGCTTCTTTTGGCGTACCGGTCGACTTCCCTCCCTCACGGCCAACCG
GTGGCAGATAACAGAGCGATCTATCCCGGGCATATCCGCCACGCTCCATGCGAATATGCC
CGCGTATTCTTGGAGGACCCGTGTAATCTGCTCCTTGAGATCCTCGGGAAGATTTGCTCC
AATTCTGACCATCCTCGAAGAATCACCCGGGTGAAGTTCGATTTCCACCGTCTCAGCCTC
GGGCTCTAGTTTCTCCTGGGTCTCTCCCTTGGTGATCTCTTGGGAGATGACATCGACCCC
CCTGGTCATTTTCTTGACTGCCCGGGCATAGCACTCCCGGGCGTTCCTCTGGTCGCCCTT
CATCTCACTCGACCA

Supp Figure 1

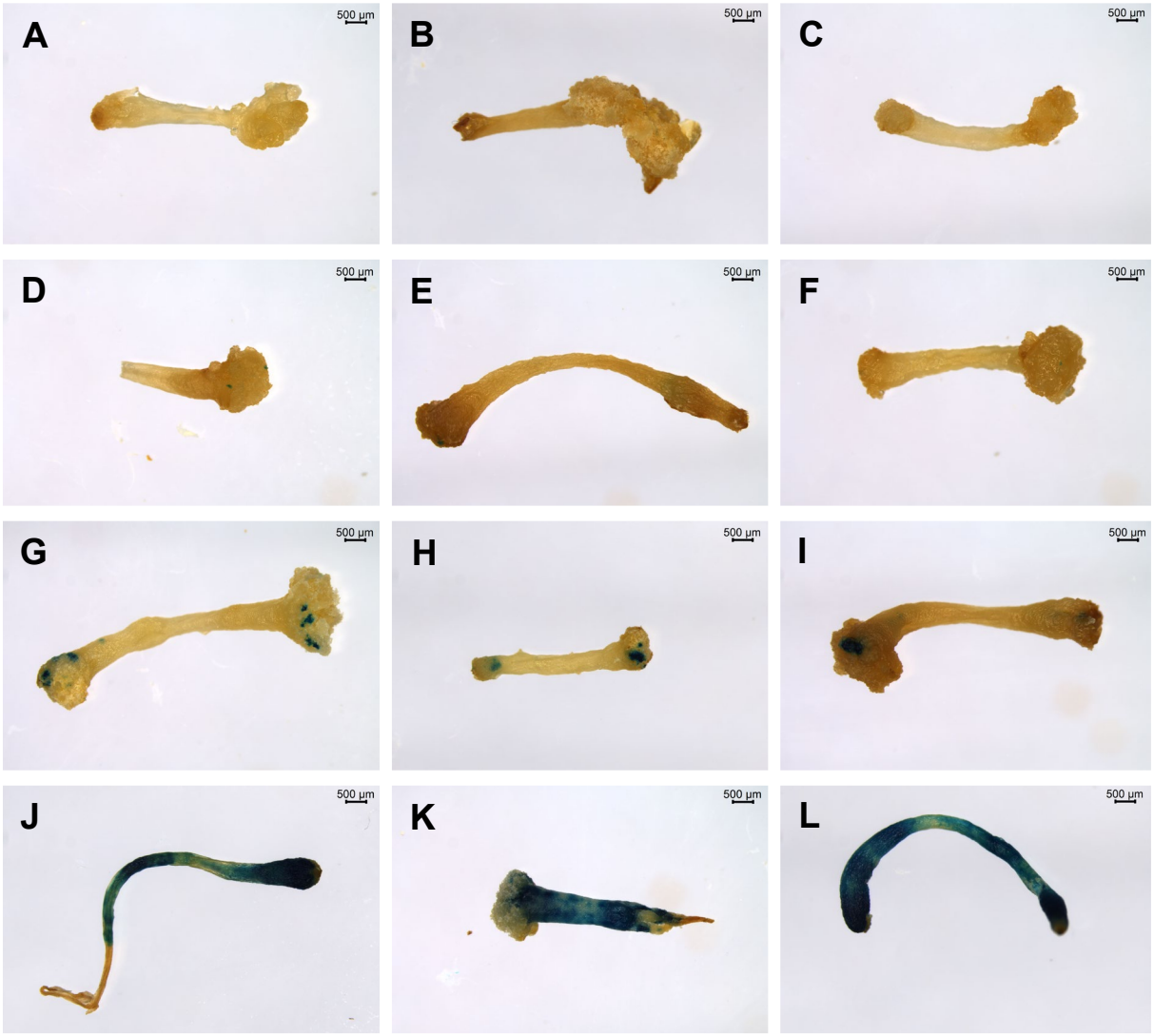

Supp Figure 2

Supplementary table 1. Media compositions for the first and second protocols.

Modified MS Media (MMS)		**Co-Cultivation Media (CCM)**		**Callus Induction Media (CIM)**	
Component	**Amount**	**Component**	**Amount**	**Component**	**Amount**
NH_4NO_3	300 mg/l	NH_4NO_3	300 mg/l	NH_4NO_3	300 mg/l
KNO_3	800 mg/l	KNO_3	800 mg/l	KNO_3	800 mg/l
$CaCl_2.2H_2O$	250 mg/l	$CaCl_2.2H_2O$	250 mg/l	$CaCl_2.2H_2O$	250 mg/l
$MgSO_4.7H_2O$	260 mg/l	$MgSO_4.7H_2O$	260 mg/l	$MgSO_4.7H_2O$	260 mg/l
KH_2PO_4	120 mg/l	KH_2PO_4	120 mg/l	KH_2PO_4	120 mg/l
H_3BO_3	6.2 mg/l	H_3BO_3	6.2 mg/l	H_3BO_3	6.2 mg/l
$MnSO_4.4H_2O$	22.3 mg/l	$MnSO_4.4H_2O$	22.3 mg/l	$MnSO_4.4H_2O$	22.3 mg/l
$ZnSO_4.7H_2O$	8.6 mg/l	$ZnSO_4.7H_2O$	8.6 mg/l	$ZnSO_4.7H_2O$	8.6 mg/l
KI	0.83 mg/l	KI	0.83 mg/l	KI	0.83 mg/l
$NaMO_4.2H_2O$	0.25 mg/l	$NaMO_4.2H_2O$	0.25 mg/l	$NaMO_4.2H_2O$	0.25 mg/l
$CuSO_4.5H_2O$	0.025 mg/l	$CuSO_4.5H_2O$	0.025 mg/l	$CuSO_4.5H_2O$	0.025 mg/l
$CoCl_2.6H_2O$	0.025 mg/l	$CoCl_2.6H_2O$	0.025 mg/l	$CoCl_2.6H_2O$	0.025 mg/l
Myo-inositol	100 mg/l	Myo-inositol	100 mg/l	Myo-inositol	100 mg/l
Nicotinic acid	1 mg/l	Nicotinic acid	1 mg/l	Nicotinic acid	1 mg/l
Pyridoxine hydrochloride	1 mg/l	Pyridoxine hydrochloride	1 mg/l	Pyridoxine hydrochloride	1 mg/l
Thiamine hydrochloride	10 mg/l	Thiamine hydrochloride	10 mg/l	Thiamine hydrochloride	10 mg/l
Glucose	3% (w/v)	Glucose	3% (w/v)	Glucose	3% (w/v)
		*Plant growth regulators		Cefotaxime	250 mg/l
				*Plant growth regulators	

* Different amounts of plant growth regulators were applied as described in the methods section.

Supplementary table 2. Media compositions for the third protocol.

Co-cultivation media (CCM)		Callus Induction Media (CIM)		Shoot Induction Media (SIM)		Shoot Elongation Media (SEM)	
Component	**Amount**	**Component**	**Amount**	**Component**	**Amount**	**Component**	**Amount**
NH_4NO_3	300 mg/l	NH_4NO_3	300 mg/l	NH_4NO_3	825 mg/l	NH_4NO_3	825 mg/l
KNO_3	800 mg/l	KNO_3	800 mg/l	KNO_3	950 mg/l	KNO_3	950 mg/l
$CaCl_2.2H_2O$	250 mg/l	$CaCl_2.2H_2O$	250 mg/l	$CaCl_2.2H_2O$	166.1 mg/l	$CaCl_2.2H_2O$	166.1 mg/l
$MgSO_4.7H_2O$	260 mg/l	$MgSO_4.7H_2O$	260 mg/l	$MgSO_4.7H_2O$	180.7 mg/l	$MgSO_4.7H_2O$	180.7 mg/l
KH_2PO_4	120 mg/l	KH_2PO_4	120 mg/l	KH_2PO_4	170 mg/l	KH_2PO_4	170 mg/l
H_3BO_3	6.2 mg/l	H_3BO_3	6.2 mg/l	H_3BO_3	6.2 mg/l	H_3BO_3	6.2 mg/l
$MnSO_4.4H_2O$	22.3 mg/l	$MnSO_4.4H_2O$	22.3 mg/l	$MnSO_4.H_2O$	16.9 mg/l	$MnSO_4.H_2O$	16.9 mg/l
$ZnSO_4.7H_2O$	8.6 mg/l	$ZnSO_4.7H_2O$	8.6 mg/l	$ZnSO_4.7H_2O$	8.6 mg/l	$ZnSO_4.7H_2O$	8.6 mg/l
KI	0.83 mg/l	KI	0.83 mg/l	KI	0.83 mg/l	KI	0.83 mg/l
$NaMO_4.2H_2O$	0.25 mg/l	$NaMO_4.2H_2O$	0.25 mg/l	$NaMO_4.2H_2O$	0.25 mg/l	$NaMO_4.2H_2O$	0.25 mg/l
$CuSO_4.5H_2O$	0.025 mg/l	$CuSO_4.5H_2O$	0.025 mg/l	$CuSO_4.5H_2O$	0.025 mg/l	$CuSO_4.5H_2O$	0.025 mg/l
$CoCl_2.6H_2O$	0.025 mg/l	$CoCl_2.6H_2O$	0.025 mg/l	$CoCl_2.6H_2O$	0.025 mg/l	$CoCl_2.6H_2O$	0.025 mg/l
Myo-inositol	100 mg/l	Myo-inositol	100 mg/l	$FeSO_4.7H_2O$	27.8 mg/l	$FeSO_4.7H_2O$	27.8 mg/l
Nicotinic acid	1 mg/l	Nicotinic acid	1 mg/l	$Na_2EDTA.2H_2O$	37.26 mg/l	$Na_2EDTA.2H_2O$	37.26 mg/l
Pyridoxine hydrochloride	1 mg/l	Pyridoxine hydrochloride	1 mg/l	Myo-inositol	100 mg/l	Myo-inositol	100 mg/l
Thiamine hydrochloride	10 mg/l	Thiamine hydrochloride	10 mg/l	Nicotinic acid	1 mg/l	Nicotinic acid	1 mg/l
Glucose	3% (w/v)	Glucose	3% (w/v)	Pyridoxine hydrochloride	1 mg/l	Pyridoxine hydrochloride	1 mg/l
NAA	3 mg/l	BAP	5 mg/l	Thiamine hydrochloride	10 mg/l	Thiamine hydrochloride	10 mg/l
BAP	1 mg/l	Cefotaxime	250 mg/l	Glucose	3% (w/v)	Glucose	3% (w/v)
				BAP	5 mg/l	BAP	5 mg/l
				Cefotaxime	250 mg/l	Cefotaxime	250 mg/l
				Timentin	100 mg/l	Timentin	100 mg/l

Supplementary table 3. TAIL-PCR conditions.

Primary TAIL-PCR	Secondary TAIL-PCR
95C – 3 min	95C – 3 min
5 cycles	5 cycles
95C – 30s	95C – 10s
62C – 1 min	64C – 1min
72C – 2:30 min	72C – 1:30min
2 cycles	15 cycles
95C – 30s	95C – 10s
25C – 3min (50% ramp)	64C – 1 min
72C – 2:30 min (32%	72C – 1:30 min
ramp)	95C -10s
	64 – 1 min
15 cycles	72C – 1:30 min
95C – 10s	95C -10s
68 – 1min	44C – 1 min
72C – 2:30 min	72C – 1:30 min
95C -10s	
68 – 1min	5 cycles
72C – 2:30 min	95C – 10s
95C – 10s	44C – 1 min
44C – 1 min	72C – 2min
72C – 2:30 min	
	72C – 5min
72C – 5min	4C 2min
4C – 2min	

Supplementary table 4. Primers used for TAIL PCR.

	Name	**Sequence 5'-3'**
T-DNA specific primers	RB1-RUBY	GTGTCCTCTCCAAATGAAATGAACTTCCTTATATAGAG
	RB2-RUBY	CCTTTGGTCTTCTGAGACTGTATCTTTGATATTCTTG
Arbitrary primers	AD1	NGTCGASWGANAWGAA
	AD2	TGWGNAGSANCASAGA
	AD3	AGWGNAGWANCAWAGG
	AD6	WGTGNAGWANCANAGA

Supplementary table 5. Primers used for cloning.

	Forward primers	**Reverse primers**
CcGRFGIF	ATGATGAGCAGTGGAAGAGGCAGG	tTTGATTCCCGCCCGCCGATC
CCWUS2	ATGGAGCCTCAACACTACTATC	tGGCGAAATGGTGAGACGAC

Supplementary table 6. Transformation efficiency on different callus induction media

NAA (mg/L)	BAP (mg/L)	TDZ (mg/L)	Plate no	Number of calli	Total explants per plate	Average of a plate	Average (%)
0	5	0	1	6	10	60	53.3
0	5	0	2	6	10	60	
0	5	0	3	5	10	50	
0	5	0	4	4	10	40	
0	5	0	5	5	10	50	
0	5	0	6	6	10	60	
0	7.5	0	1	5	10	50	56.7
0	7.5	0	2	5	10	50	
0	7.5	0	3	7	10	70	
0	7.5	0	4	6	10	60	
0	7.5	0	5	4	10	40	
0	7.5	0	6	7	10	70	
0	10	0	1	3	10	30	31.7
0	10	0	2	3	10	30	
0	10	0	3	4	10	40	
0	10	0	4	4	10	40	
0	10	0	5	2	10	20	
0	10	0	6	3	10	30	
0	25	0	1	6	10	60	43.3
0	25	0	2	5	10	50	
0	25	0	3	6	10	60	
0	25	0	4	5	10	50	
0	25	0	5	2	10	20	
0	25	0	6	2	10	20	
0	0	0.05	1	5	10	50	43.3
0	0	0.05	2	3	10	30	
0	0	0.05	3	4	10	40	
0	0	0.05	4	6	10	60	
0	0	0.05	5	3	10	30	
0	0	0.05	6	5	10	50	

0	0	0.1	1	7	10	70	36.7
0	0	0.1	2	2	10	20	
0	0	0.1	3	3	10	30	
0	0	0.1	4	5	10	50	
0	0	0.1	5	3	10	30	
0	0	0.1	6	2	10	20	
0	0	0.3	1	2	10	20	33.3
0	0	0.3	2	4	10	40	
0	0	0.3	3	2	10	20	
0	0	0.3	4	4	10	40	
0	0	0.3	5	4	10	40	
0	0	0.3	6	4	10	40	
0	0	0.5	1	6	10	60	50.0
0	0	0.5	2	5	10	50	
0	0	0.5	3	6	10	60	
0	0	0.5	4	7	10	70	
0	0	0.5	5	5	10	50	
0	0	0.5	6	1	10	10	
0.5	5	0	1	5	10	50	26.7
0.5	5	0	2	2	10	20	
0.5	5	0	3	4	10	40	
0.5	5	0	4	3	10	30	
0.5	5	0	5	2	10	20	
0.5	5	0	6	0	10	0	
0.5	7.5	0	1	2	10	20	26.7
0.5	7.5	0	2	2	10	20	
0.5	7.5	0	3	3	10	30	
0.5	7.5	0	4	3	10	30	
0.5	7.5	0	5	3	10	30	
0.5	7.5	0	6	3	10	30	
0.5	10	0	1	1	10	10	31.7
0.5	10	0	2	4	10	40	
0.5	10	0	3	5	10	50	
0.5	10	0	4	4	10	40	
0.5	10	0	5	2	10	20	

0.5	10	0	6	3	10	30	
0.5	25	0	1	1	10	10	13.3
0.5	25	0	2	1	10	10	
0.5	25	0	3	2	10	20	
0.5	25	0	4	1	10	10	
0.5	25	0	5	2	10	20	
0.5	25	0	6	1	10	10	
0.5	0	0.05	1	5	10	50	26.7
0.5	0	0.05	2	2	10	20	
0.5	0	0.05	3	3	10	30	
0.5	0	0.05	4	2	10	20	
0.5	0	0.05	5	3	10	30	
0.5	0	0.05	6	1	10	10	
0.5	0	0.1	1	1	10	10	16.7
0.5	0	0.1	2	2	10	20	
0.5	0	0.1	3	1	10	10	
0.5	0	0.1	4	3	10	30	
0.5	0	0.1	5	2	10	20	
0.5	0	0.1	6	1	10	10	
0.5	0	0.3	1	2	10	20	33.3
0.5	0	0.3	2	5	10	50	
0.5	0	0.3	3	3	10	30	
0.5	0	0.3	4	4	10	40	
0.5	0	0.3	5	2	10	20	
0.5	0	0.3	6	4	10	40	
0.5	0	0.5	1	3	10	30	25.0
0.5	0	0.5	2	1	10	10	
0.5	0	0.5	3	2	10	20	
0.5	0	0.5	4	3	10	30	
0.5	0	0.5	5	3	10	30	
0.5	0	0.5	6	3	10	30	
0	0	0	1	2	10	20	8.3
0	0	0	2	2	10	20	
0	0	0	3	1	10	10	
0	0	0	4	0	10	0	

0	0	0	5	1	10	10
0	0	0	6	1	10	10
0	0	0	1	0	10	0
0	0	0	2	1	10	10
0	0	0	3	0	10	0
0	0	0	4	0	10	0
0	0	0	5	1	10	10
0	0	0	6	1	10	10

Supplementary table 7. Different transformation efficiency between the cut and the bulk chop method. DAI is days after inoculation.

Wounding method	Incubation dates	Total explants per plate	Replicates					Average number of red spots in a plate	Average efficiency (%)
			plate 1	plate 2	plate 3	plate 4	plate 5		
Cut	20 DAI	10	10	10	10	10	10	10	100
Chop	20 DAI	20	15	17	10	9	14	13	65

Supplemental table 8. Transformation efficiency with RUBY reporter. Number of segments expressing RUBY were scored from 4DAI to 45 DAI. Sixteen independent biological repeats were performed (n=50). DAI: Days after Agro inoculation.

No. of reps.	5 DAI (%)	15 DAI (%)	25 DAI (%)	35 DAI (%)	45 DAI (%)
1	100	88.0	82.0	78.0	68.0
2	100	88.5	80.8	76.9	69.2
3	100	94.6	80.4	73.2	60.7
4	100	92.3	82.7	69.2	65.4
5	100	98.0	84.0	74.0	50.0
6	100	100.0	94.0	82.0	60.0
7	100	88.1	78.0	74.6	45.8
8	100	98.1	94.2	78.8	57.7
9	100	94.0	94.0	80.0	80.0
10	100	90.0	90.0	74.0	74.0
11	100	84.0	80.0	74.0	62.0
12	100	96.0	94.0	74.0	72.0
13	100	94.7	86.0	84.2	52.6
14	100	96.2	90.4	88.5	65.4
15	100	96.2	84.6	73.1	53.8
16	100	92.9	80.4	73.2	57.1
Average	100	93.2	86.0	76.7	62.1

Supplemental table 9. Transformation efficiency with RUBY reporter. Number of callus expressing RUBY, number of shoots expressing RUBY and number of RUBY *Cuscuta* coiled on a host were counted. Eight independent biological repeats were performed (n=50).

No. of reps.	% of callus on Shoot elongation	% of callus producing shoot	% of shoots coiled on a host
1	24.0	10.0	8.0
2	14.0	4.0	4.0
3	12.0	4.0	2.0
4	24.0	8.0	4.0
5	18.0	8.0	2.0
6	6.0	0.0	0.0
7	10.0	0.0	0.0
8	20.0	8.0	2.0
Average	16.0	5.3	2.8